RSC Advances

Preparation and Characterization of Chitosan/Silver Nanoparticles /Copper Nanoparticles/Carbon Nanotubes Multifunctional Nano-Composite for Water Treatment: (1) Heavy Metals Removal; Kinetics, Isotherms and Competitive Studies

Preparation and Characterization of Chitosan/Silver Nanoparticles /Copper Nanoparticles/Carbon Nanotubes Multifunctional Nano-Composite for Water Treatment: (1) Heavy Metals Removal; Kinetics, Isotherms and Competitive Studies

Ahmed M. Alsabagh, M. Fathy, Rania E. Morsi[*]

Egyptian Petroleum Research Institute, Nasr City, P.B. 11727, Cairo, Egypt

Abstract

In this work, a multifunctional nanocomposite of chitosan, silver nanoparticles (Ag NPs), copper nanoparticles (Cu NPs) and carbon nanotubes (CNTs) has been successfully prepared. The structure has been confirmed using X-ray diffraction, scanning and transmittance electron microscopes. CNTs, Ag NPs and Cu NPs are distributed homogeneously inside the polymer matrix. The adsorption efficiency of chitosan for Cu(II), Cd(II) and Pb(II) reached 60% using 5 g/L adsorbent dose while for the multifunctional composite, it reached 100% adsorption efficiency with reduction of the amount of adsorbent to 1 g/L. The contact time required for equilibrium was 10 min. For the multifunctional composite, 10 min is enough for almost complete removal of metal ions from the solution while for chitosan, the efficiency is rather lower. The adsorption process fitted to the pseudo-second order kinetic model and Langmuir isotherm in the linear form in case of chitosan while in case of the multifunctional composite, it fitted to the pseudo-second order kinetic model and Langmuir and Freundlich models in the non-linear forms. The maximum amount adsorbed (Q_{max}) was found to be directly related and much fitted with the electrode potential values of metal ions in case of chitosan while for the multifunctional composite, ionic radius is the most dependent parameter. The multifunctional composite was found to be regenerated effectively using EDTA solution up to five efficient cycles of adsorption/desorption processes.

---

[*] Corresponding author: raniaelsayed@yahoo.com

Keywords

Chitosan, Silver Nanoparticles, Copper Nanoparticles, Carbon Nanotubes, Multifunctional Composites, Water Treatment, Heavy Metals Removing, Adsorption/Desorption Process, Recycling.

1- Introduction

Heavy metal ions constitute one of the most dangerous water soluble pollutants. Exposure to low concentrations of heavy metal ions may provoke loss of weight, audition, diarrhea, muscular weakness, growth retardation, cardiovascular abnormalities, cancers, renal insufficiency and sleeping disturbances[1,2]. The importance of water, sanitation and hygiene for health and development has been reflected in the outcomes of a series of international policy forums. EPA stated that maximum contaminant level (MCL) for Cadmium is 0.05 ppm while for copper, the action level is 1.3 mg/L and for lead is 0.015 mg/L[3].

For heavy metal removal, different technologies and processes are currently used. Biological treatments [4-6], membrane processes [7-9] and adsorption procedures [10-12] are the most widely used for removing metals and organic compounds from industrial effluents. Amongst all the treatments proposed, adsorption is a well-known separation process. It is now recognized as an effective, efficient and economic method for water decontamination applications. Eco-friendly natural polymers as chitin, chitosan[13,14] and their derivatives[15,16] are of great potential. Chitosan, a polysaccharide biopolymer obtained from the deacetylation of chitin, has been widely used in many applications because it can not only be economically processed from chitin but is also nontoxic, biocompatible and biodegradable[17,18]. Chitosan is known to have a good complexing ability through specific interactions of its amino groups with heavy metals[19-23]. Chitosan modification is of significant interest due to the expected exceptional properties and applications. Among the materials used for such modification; carbon nanotubes (CNTs) have captured much attention worldwide since its discovery in 1991[24]. CNTs have unique size distributions, hollow-tube structures and high specific surface areas. These

characteristics allow applications of CNTs in many fields[25-32]. Many research studies have shown the capability of CNTs in the adsorption and removal of different pollutants; it showed a superior efficiency in removal of, for example, Cr[33], Pb[34], Cd[35], Cu[36] , etc... On the other hand, several natural and engineered nanomaterials have also been shown to have strong antimicrobial properties, including chitosan[37], silver nanoparticles[38], Copper nanoparticles[39] and Carbon nanotubes[40]. Unlike conventional chemical disinfectants, these antimicrobial nanomaterials are not strong oxidants and are relatively inert in water. Therefore, they are not expected to produce harmful disinfection byproducts. If properly incorporated into treatment processes, they have the potential to replace or enhance conventional disinfection methods.

In this work, a multifunctional composite of chitosan/Ag NPs/Cu NPs/CNTs, that can clean water effectively from heavy metal and microbes, was prepared as active material that can be used in filter technology and purification systems. In this part of the work, the prepared multifunctional composite was evaluated for heavy metals removal. Cu(II), Cd(II) and Pb(II) were used as representative examples for heavy metal contaminates in waste water. The adsorption kinetics, isotherms and competitive studies were carried out. A correlation between the maximum uptake capacity and the electrochemical properties of the studied metal ions and the adsorption/desorption processes were also highlighted.

2- Materials & Methods

2.1. Materials

Chitosan was extracted from marine shrimp waste materials and was found to have a degree of deacetylation of 85% as determined with potentiometric titration and molecular weight of 2122 kDa as determined from the intrinsic viscosity measurement. Multiwall carbon nanotubes (CNTs) with an average diameter 60 to110 nm were kindlysupplied from EPRI nanotechnology center. Silver nanoparticles and copper nanoparticles used were of average particle size 40-60 nm. Analytical grade lead chloride, copper chloride and cadmium chloride were used to prepare stock solutions of

1000 mgL^{-1} of the three metal ions, which were further diluted to the required concentrations before use. All other reagents were of analytical grade and used as received without further purification.

2.2. Preparation of the multifunctional-composite

Chitosan/Ag NPs/Cu NPs/CNTs multifunctional composite was prepared using equal weights of Ag NPs, Cu NPs and CNTs in a total ratio of 5 wt% of nano materials with respect to chitosan. Chitosan was dissolved in 2% acetic acid to prepare 1% polymer solution and filtered to remove any remaining impurities. CNTs, Ag NPs and Cu NPs, each one was dispersed individually in ethanol by sonication for 20 min and added dropwisely to the previously prepared chitosan solution under stirring. The mixture was stirred for 4 h in a rotation speed of 500 rpm and the formed composite was further sonicated for 30 min for homogenization. The composite was then precipitated in a mixture of NaOH solution and ethanol, filtered, washed several times with deionized water until colorless filtrate was obtained with neutral pH and finally vacuum dried at 60 °C and 850 mb to constant weight. The yield was about 95% of the total starting weights.

2.3. Characterization of the prepared multifunctional composite

The composite was characterized by powder X-ray diffraction (XRD) using a Philips X'Pertpro Pan-analytical instrument. Data was taken for the 2θ range of 10 to 80 degrees with a step of 0.02 degree. Transmission Electron Microscopy (TEM) imaging was performed using a Jeol-JEM Japan 2100 operating at 200 kV, the samples were prepared for imaging by sonication of samples in ethyl alcohol and depositing onto a copper coated carbon grid and then let the solvent to evaporate. The Scanning Electron Microscope imaging was performed using SEM Model Quanta 250 FEG (Field Emission Gun) attached with EDX Unit (Energy Dispersive X-ray Analyses), FEI, Netherlands.

2.4. Metal uptake

Assessment of metal ions adsorption is carried out by batch adsorption experiments. Batch mode sorption experiments were performed in sealed glass flasks at room temperature. In a primary experiment, bi-composites of chitosan with individual Cu NPs, Ag NPs and CNTs was investigated as Cu(II), Cd(II) and Pb(II) metal ions adsorbents. Pre-weighted amounts of the composites were added to a glass flasks contain 20 ml of the desired concentration of aqueous metal solution. The glass flasks were stirred for the desired time, filtered and then the metal ions concentrations were measured. The effects of the composite dosage (in the range from 0.5 g/L to 5 g/L), contact time (1 to 90 min) and the initial metal ions concentrations (10 to100 ppm) for Cu(II), Cd(II) and Pb(II) metal ions were investigated. The amount of metal ions adsorbed on the composite was determined by the difference of the initial concentration (C_i) and the equilibrium concentration (C_e). The percentage removed of metal ions was calculated as following:

$$removal\ (\%) = \frac{C_i - C_e}{C_i} \times 100 \tag{1}$$

The adsorption capacity (q_e) was calculated as following:

$$q_e(mg/g) = \frac{C_i - C_e}{M} \times V \tag{2}$$

where, V = volume of the metal ion solution (L), M = weight of adsorbent (g).

More analysis of the experimental data was performed using four common kinetics model equations to find the best-fitted model for the obtained data. The kinetic models used are pseudo-first order, 1st order, pseudo-second order and 2nd order kinetic models[41]. In addition, the experimental adsorption data were fitted according to different adsorption isotherms; Langmuir, Freundlich, Temkin and Dubinin-Radushkevich isotherms.

3- Results and Discussion

3.1. Characterization of chitosan/ Ag NPs/ Cu NPs/CNTs multifunctional composite

Figure 1 represents the microscopic images of chitosan/Ag NPs/Cu NPs/CNTs multifunctional composite and its individual components. The images reveal that carbon nanotubes are attached to chitosan matrix and the spherical Cu NPS and Ag NPs in the range of 40-60 nm are embedded inside changing the overall morphology. The multifunctional composite form a characteristic polymer based matrix due to the presence and combination of different shapes; spherical NPs and nanotubes as represented in Scheme 1.

Figure 1a) TEM images of Ag NPs (right) Cu NPs (middle) and MWCNTs (left), b) TEM image of the multifunctional composite; the insertion is for higher magnification image and c) SEM image of the multifunctional composite; the insertion is for higher magnification image.

Scheme 1: Schematic representation of the different active sites of the prepared multifunctional composite.

Figure 2 represents the X-ray diffraction pattern of the multifunctional composite; peak observed $2\theta=20°$ corresponds to a hydrated structure and an amorphous structure of chitosan[42,43]. The expected peak at $2\theta = 25°$ correspond to CNTs was found to be overlapped with the broad amorphous peak of chitosan due to the interaction between them. The characteristic peaks of Ag NPs were found at $2\theta=38.58°$ and $2\theta=44.68°$while for Cu NPs, peak at $2\theta=43.64°$ have been observed[44].

Figure 2: XRD of the prepared multifunctional composite.

3.2. Uptake capacity of the bi-composites in comparison with bare chitosan and the multifunctional composite.

In a primary experiment, bi-composites of chitosan with individual Cu NPs, Ag NPs and CNTs was investigated as Cu(II), Cd(II) and Pb(II) metal ions adsorbents and the results are shown in Figure 3 which reveals that the uptake efficiency of the multifunctional composite is superior to that of chitosan and is higher than that of the bi-composites systems.

Figure 3: comparison study of the uptake capacity of chitosan, chitosan/Cu NPs nanocomposite, chitosan/Ag NPs nanocomposite, chitosan/CNTs nanocomposite and chitosan/ Ag NPs/ Cu NPs/CNTs multifunctional composite regarding Cu(II), Cd(II) and Pb(II)metal ions (100 ppm, 1h, 3 g/L).

3.3. Metals uptake of chitosan/ Ag NPs/ Cu NPs/ CNTs multifunctional composite

3.3.1. Effect of adsorbent dose

The optimum amount of the adsorbent required for quantitative removal of 100 ppm of metal ions (Cu(II), Cd(II) and Pb(II)) was determined by investigating different adsorbent doses. Five different weights of the multifunctional composite were used; 0.01, 0.02, 0.04, 0.06 and 0.1g which represent the adsorbent concentration of 0.5, 1, 2, 3 and 5 g/L and were compared to the adsorption of the equivalent weights of chitosan as shown in Figure 4.

For chitosan, the adsorption efficiency of the three investigated metals is generally enhanced when the amount of chitosan increased reaching 60% using 5 g/L. This can be attributed to the increased availability of adsorption sites. The sorption mechanism was mainly attributed to interactions between the metal ions and functional groups in chitosan. For the multifunctional composite, it reached 100% adsorption efficiency using only 1 g/L. This may be attributed to interactions between the metal ions and binding sites of chitosan, CNTs (the surface functional groups, the multilayer and the hollow area inside the tubes) and the produced matrix of the multifunctional

composite as detected from the microscopic image shown in Figure 1 and represented in scheme 1. The comparison of multifunctional composite with other adsorbents suggests that multifunctional composite have a great potential toward the heavy metals removal.

Figure 4: Effect of adsorbent dose of chitosan and the multifunctional composite keeping the concentration at 100ppm for 60min.

3.3.2. Effect of contact time and the kinetic studies

Different contact times between the multifunctional composite and metal ions were investigated from 1 up to 90 min. Results are shown in Figure 5. Generally, contact time of 10 min was enough for maximum adsorption efficiency. In case of the multifunctional composite, these 10 min is enough for almost complete removal of metal ions from the solution while for chitosan the efficiency was rather lower.

For further analysis of the results, several kinetic models are investigated to describe the adsorption kinetics. In this study, four common equations were tested to find the best-fitted model for the experimental data obtained from the adsorption of different metal ions.

The pseudo-first order kinetic model was suggested by Lagergren[45] for the adsorption of solid/liquid systems and its linear form can be formulated as:

$$Ln(q_e - q_t) = \frac{Ln(q_e) - K_{1p}t}{2.303} \tag{3}$$

The first order kinetic model in linear form can be formulated as:

$$Log\frac{q_e - q_t}{q_e} = \frac{K_1 t}{2.303} \tag{4}$$

Ho and McKay's pseudo-second order kinetic model[46] can be expressed as:

$$\frac{t}{q_t} = \frac{1}{2k_{2p}q^2_e} + \frac{t}{q_e} \tag{5}$$

The second order kinetic model in linear form can be formulated as:

$$\frac{1}{q_e - q_t} = \frac{1}{q_e} + k_2 t \tag{6}$$

where q_e and q_t are the amount of metal ion adsorbed (mgg^{-1}) at equilibrium and at time t, respectively. k_{1p} is the equilibrium rate constant of the pseudo-first order adsorption (min^{-1}). k_1 is the equilibrium rate constant of the first order adsorption (min^{-1}). k_{2p} is the equilibrium rate constant of the pseudo-second order adsorption ($gmg^{-1}min^{-1}$).k_2 is the equilibrium rate constant of the second order adsorption ($g^{-1}mg^{-1}min^{-1}$).

The experimental data have been fitted by the mentioned kinetics models. Based on the analysis of the R^2 of the linear form for various kinetics models, as shown in Table 1, the pseudo-second order model was more appropriate to describe the adsorption kinetics behaviors for Cu(II), Cd(II) and Pb(II) ions onto chitosan and the multifunctional composite. The fitting of the experimental data to the pseudo-second order model was shown in Figure 6.

Figure 5: Uptake capacity of the multifunctional composite over time (3g/L, 100ppm).

Figure 6: Adsorption kinetics pseudo-second order model of Cu(II), Cd(II) and Pb(II) ions on chitosan and the multifunctional composite.

Table 1: Kinetics parameters for Cu(II), Cd(II), Pb(II) ions adsorption.

3.3.3. Effect of initial metal ion concentration and the adsorption isotherms

From Figure 7, the uptake capacity of the multifunctional composite increases with the increase of the initial metal ions concentration while chitosan almost reach maximum uptake that barely increase with increase metal ions concentration. The analysis of the adsorption process requires the relevant adsorption equilibrium, which is the most important piece of information in understanding an adsorption process.

Adsorption equilibrium provides the fundamental physicochemical data for evaluating the applicability of the adsorption process[47]. Figure 8 shows the adsorption equilibrium isotherm obtained for metal ions adsorption onto chitosan and the multifunctional composite. The figure represents the relationship between the amount of metal ion adsorbed onto the adsorbent and the remaining metal ion concentration in the aqueous phase at equilibrium. The adsorption capacity was found to increase with the equilibrium concentration of the metal ion in solution, progressively reaching saturation of the adsorbent.

Figure 7: Effect of initial concentration of Cu(II), Cd(II) and Pb(II) ions on chitosan and multifunctional composite uptake capacity(3g/L, 60min).

For further analysis of the results, several common isotherm equations were tested to find the best-fitted adsorption isotherm model for the experimental data obtained of Cu(II) ions as a representative example.

Langmuir isotherm: the experimental adsorption data were fitted according to the Langmuir isotherm model, equation 7 being preferentially used for studies on adsorption in solution[48].

$$q_e = \frac{K_L C_e q_m}{1 + K_L C_e} \tag{7}$$

where q_e and C_e are the amount adsorbed (mgg^{-1}) and the adsorbate concentration in solution (mgL^{-1}), respectively, both at equilibrium. K_L is the Langmuir constant (Lmg^{-1}) and q_m is the maximum adsorption capacity of the monolayer formed on the adsorbent (mgg^{-1}).

Langmuir model assumes that the adsorbent surface has sites of identical energy and that each adsorbate molecule is located at a single site; hence, it predicts the formation of a monolayer of the adsorbate on the adsorbent surface[49]. The linear form of the Langmuir isotherm, represented by equation 8, is employed to determine the q_m and

K_L values from the angular and linear coefficients obtained by plotting C_e/q_e as a function of C_e which are given in Table 2.

$$\frac{C_e}{q_e} = \frac{1}{K_L q_m} + \frac{C_e}{q_m} \tag{8}$$

Fitting of Langmuir isotherm suggests forming monolayer of metal ions on some of the material binding sites.

Freundlich isotherm: the Freundlich isotherm is an empirical equation employed to describe equilibrium on heterogeneous surfaces and hence does not assume monolayer capacity. Mathematically, it is expressed by

$$q_e = K_f C^{1/n} \tag{9}$$

Equation 9 can also be expressed in the linearized logarithmic form as

$$Log q_e = Log K_f + \frac{1}{n} Log C_e \tag{10}$$

where K_f and n are the Freundlich isotherm constants indicating the adsorption capacity (mgg^{-1}) and adsorption intensity (unitless), respectively[50,51].

Fitting of Freundlich isotherm suggests the presence of different binding sites in the investigated materials.

Temkin isotherm: Temkin adsorption isotherm was developed assuming that the heat of adsorption of all the molecules decreases linearly with coverage because adsorbate–adsorbate interaction is characterized by a uniform distribution of binding energies up to some maximum binding energy. Temkin isotherm is represented by the following equation:

$$q_e = \frac{RT}{b} Log(K_T C_e) \tag{11}$$

Equation 11 can be expressed in its linear form as:

$$q_e = B_T Log K_T + B_T Log C_e \tag{12}$$

where B_T: $\frac{RT}{b}$ *(Temkin constant related to the heat of adsorption (KJmol[-1])), R is the gas constant (8.314 Jmol[-1]K[-1]), T is the temperature (K) and K_T is the empirical Temkin constant related to the equilibrium binding constant and to the maximum binding energy.*

Dubinin-Radushkevich isotherm: the equilibrium data were further tested with the Dubinin-Radushkevich isotherm model (D-R isotherm). This isotherm model predicts the nature of the adsorbate sorption onto the adsorbent and it is used to calculate the mean free energy of sorption. The non-linear D-R isotherm is expressed as:

$$q_e = q_m \exp(-K \in^2) \tag{13}$$

and the linearized form of the equation is given as:

$$Ln q_e = Ln q_m - k \in^2 \tag{14}$$

where q_e is the amount of solute adsorbed per mass of adsorbent (mgg[-1]), q_m is the maximum adsorption capacity (mgg[-1]), k is the D-R constant (mol[2]kJ[-2]) and $\in$ is the Polanyi potential (Jmol[-1]), which can be calculated as:

$$\in = RTLn\left(1 + \frac{1}{C_e}\right) \tag{15}$$

where R is the gas constant (J mol^{-1}K[-1]), T is the absolute temperature (K) and C_e is the equilibrium concentration of the adsorbate in aqueous solution (gL[-1]) [52,53]. The values of q_m and k were calculated and are shown in Table 2.

The mean free energy of adsorption (E) was calculated from the k values using the equation:

$$E = \frac{1}{\sqrt{2K}} \tag{16}$$

The E value is used to ascertain the type of adsorption process under consideration. If this value is between 8 and 16 kJ mol^{-1}, the adsorption process can be assumed to involve chemical sorption and values lower than 8 kJ mol^{-1} indicate that the adsorption process is of a physical nature[54,55].

On analyzing the values of R^2 obtained using three isotherm models, it can be observed that the Langmuir equation in the linear form provided the best fit for the experimental data in case of chitosan while Freundlich model in the non-linear form provided the best fit for the experimental data in case of the multifunctional composite.

Figure 8: Cu(II) adsorption isotherms fitting of chitosan and multifunctional composite (3g/L, 60min).

Table 2: Isotherms parameters of Cu (II) adsorption on chitosan and the multifunctional composite.

3.3.4. Correlation between the maximum uptake capacity and the electrochemical properties of metal ions

Competitive adsorption is important in water and waste water treatment because most metal ions to be adsorbed exist in solution with other metal ions. Even though all the studied metals are bivalent, the differences in the capacity and thus interactions with the adsorption centers are obvious. There is no consensus between the researchers regarding the competitive adsorption of metal ions. They commonly related to the properties of these ions in aqueous solution, which may affect the energy of surface binding and interactions. Another factor is the accessibility of adsorption centers, which also can be linked to the sizes of species to be adsorbed and their effective charge. According to Park and Kim[56] and Horsfall and Spiff[57], the adsorption of heavy metal ions should depend on the ionic radius of adsorbate. For instance, the large ionic radius should decrease adsorption due to the steric effects. Gabaldon et al. found that during multi-component adsorption, various metal ions occupy the specific number of surface sites, which decreases the removal efficiency of the adsorbent for the metals of interest[58]. Ücer et al. proposed that the electro-negativity plays an important role in competitive

adsorption[59]. On the other hand, Allen and Brown interpreted the multi-component isotherm systems as dependent on one or all of the following parameters: ionic radius, electronegativity and ionization energy[60]. It is well known that surface physical adsorption (related to the surface area), ion exchange and redox properties (related to functional groups)[61] can be involved into heavy metal adsorption in solution.

In our experiments, plotting the dependence of the amount adsorbed (Q_{max}) against standard electrode potential values reveals the most fitted linear trend in case of chitosan while for the multifunctional composite, ionic radius is the most dependent parameter among the investigated electrochemical parameters. These relations are represented Figure 9 and the R^2 values of the different parameters are summarized in Table 3. Accordingly, it appears that the adsorption for the multifunctional component is mainly physical adsorption and related to the surface properties, while for chitosan the adsorption is mainly according to redox properties and depend on its functional groups.

Figure 9: The most fitted electrochemical parameters of Cu(II)*, Cd*(II) *and Pb*(II) *in relation to maximum uptake capacity of chitosan and the multifunctional composite.*

Table 3: R^2 values of the relation between the maximum uptake capacity and the electrochemical parameters of the used metal ions.

3.3.5. Recycling and desorption

Desorption studies are important to investigate the possibility for the recovery of metals adsorbed on the adsorbent surface as well as for the regeneration of the adsorbent for subsequent reuse. In this study, H_2O, 0.1M EDTA were used as eluents. Using H_2O as eluent showed almost no desorption efficiency and this is ideal for filter material so that the adsorbed metal ions can't be eluted by water stream. 0.1M EDTA solution showed high desorption efficiency and the multifunctional composite regenerate its adsorption efficiency even after several washing cycles. Figure 10 shows five cycles of

adsorption/desorption process in which, after the first cycle, the adsorption/desorption efficiency remains almost constant.

Figure 10: Adsorption / desorption cycles of the multifunctional composite using Cu (II) as adsorbate and EDTA as eluting agent.

Conclusion

Multifunctional nanocomposite of chitosan, silver nanoparticles, copper nanoparticles and carbon nanotubes can be prepared and effectively used in water treatment. X-ray diffraction, scanning and transmittance electron microscopes confirmed the distribution of CNTs, Ag NPs and Cu NPs in the polymer matrix. The prepared multifunctional nanocomposite has a superior Cu(II), Cd(II) and Pb(II) adsorption efficiency comparing with chitosan and the bi-nanocomposites systems.

The comparison of multifunctional composite with chitosan suggests that multifunctional composite have much higher potential toward the heavy metals removal. For chitosan, the adsorption efficiency of Cu(II), Cd(II) and Pb(II) reached 60% using 5 g/L while for the multifunctional composite, it reached 100% adsorption efficiency using only 1 g/L. Contact time of 10 min was enough for almost complete removal of metal ions from the solution using the multifunctional composite.

The adsorption process was found to follow the pseudo second order kinetic model and Langmuir isotherm in case of chitosan. For the multifunctional composite, the process follows the pseudo second order kinetic model and Freundlich isotherm.

The maximum amount adsorbed (Q_{max}) was found to be directly related and much fitted with the electrode potential values of metal ions in case of chitosan while for the multifunctional composite, ionic radius is the most dependent parameter.

The multifunctional composite was found to be regenerated effectively using EDTA solution up to five efficient cycles of adsorption/desorption processes.

The presented work suggests the multifunctional composite as a promising water purification material.

Further work is being carried out for the antimicrobial activity of the multifunctional composite and for using a carrier for the multifunctional composite to get lower cost efficient purification matrix.

Acknowledgement

References

1. Pereira, Luciano de Almeida, de Amorim, Ilmair Gonçalves and da Silva, José Bento Borba, *Talanta*, 2004, **64**(2), 395.

2. Q. W. Yang, W. S. Shu, J. W. Qiu, H. B. Wang and C. Y. Lan, *Environment International*, 2004, **30**(7), 883.

3. Water.epa.gov/drink/contaminants/upload/mcl-2.pdf.

4. C. I. Pearce, Lloyd, JR and J. T. Guthrie, *Dyes and pigments*, 2003, **58**(3), 179.

5. G. McMullan, C. Meehan, A. Conneely, N. Kirby, T. Robinson, P. Nigam, I. Banat, R. Marchant and W. Smyth, *Applied Microbiology and Biotechnology*, 2001, **56**(1-2), 81.

6. Y. Fu and T. Viraraghavan, *Bioresource technology*, 2001, **79**(3), 251.

7. Van der Bruggen, Bart and C. Vandecasteele, *Environmental pollution*, 2003, **122**(3), 435.

8. A. Cassano, R. Molinari, M. Romano and E. Drioli, *Journal of Membrane Science*, 2001, **181**(1), 111.

9. V. V. Goncharuk, D. D. Kucheruk, V. M. Kochkodan and V. P. Badekha, *Desalination*, 2002, **143**(1), 45.

10. Z. Hu, L. Lei, Y. Li and Y. Ni, *Separation and purification technology*, 2003, **31**(1), 13.

11. J. Rivera-Utrilla, I. Bautista-Toledo, M. A. Ferro-Garcıa and C. Moreno-Castilla, *Carbon*, 2003, **41**(2), 323.

12. I. L. Lagadic, M. K. Mitchell and B. D. Payne, *Environmental science & technology*, 2001, **35**(5), 984.

13. J. Synowiecki and N. A. Al-Khateeb, 2003.

14. Ravi Kumar, Majeti NV, *Reactive and Functional Polymers*, 2000, **46**(1), 1.

15. S. Babel and T. A. Kurniawan, *Journal of Hazardous Materials*, 2003, **97**(1), 219.

16. A. J. Varma, S. V. Deshpande and J. F. Kennedy, *Carbohydrate Polymers*, 2004, **55**(1), 77.

17. V. K. Mourya and N. N. Inamdar, *Reactive and Functional Polymers*, 2008, **68**(6), 1013.

18. M. Rinaudo, *Progress in polymer science*, 2006, **31**(7), 603.

19. K. Z. Elwakeel, *Desalination*, 2010, **250**(1), 105.

20. A. Gamage and F. Shahidi, *Food Chemistry*, 2007, **104**(3), 989.

21. N. G. Kandile and A. S. Nasr, *Carbohydrate Polymers*, 2009, **78**(4), 753.

22. M. Rhazi, J. Desbrieres, A. Tolaimate, M. Rinaudo, P. Vottero and A. Alagui, *Polymer*, 2002, **43**(4), 1267.

23. M. Rhazi, J. Desbrieres, A. Tolaimate, M. Rinaudo, P. Vottero, A. Alagui and M. El Meray, *European Polymer Journal*, 2002, **38**(8), 1523.

24. S. Iijima, *nature*, 1991, **354**(6348), 56.

25. S.-u. Rather, S. W. Hwang, A. R. Kim and K. S. Nahm, *Journal of Alloys and Compounds*, 2009, **475**(1), L17.

26. K.-J. Lee, M.-H. Hsu, H.-Z. Cheng, J. S.-C. Jang, S.-W. Lin, C.-C. Lee and S.-C. Lin, *Journal of Alloys and Compounds*, 2009, **483**(1), 389.

27. N. de Jonge, *Advances in imaging and electron physics*, 2009, **156**, 203.

28. S. Darbari, Y. Abdi, S. Mohajerzadeh and E. Asl Soleimani, *Carbon*, 2010, **48**(9), 2493.

29. I. P. Jain, P. Jain and A. Jain, *Journal of Alloys and Compounds*, 2010, **503**(2), 303.

30. W. Cheung, F. Pontoriero, O. Taratula, A. M. Chen and H. He, *Advanced drug delivery reviews*, 2010, **62**(6), 633.

31. S. Hermann, B. Pahl, R. Ecke, S. E. Schulz and T. Gessner, *Microelectronic Engineering*, 2010, **87**(3), 438.

32. C.-H. Chen, Y.-H. Liang and W.-D. Zhang, *Journal of Alloys and Compounds*, 2010, **501**(1), 168.

33. J. Hu, C. Chen, X. Zhu and X. Wang, *Journal of Hazardous Materials*, 2009, **162**(2), 1542.

34. Y.-H. Li, S. Wang, J. Wei, X. Zhang, C. Xu, Z. Luan, D. Wu and B. Wei, *Chemical Physics Letters*, 2002, **357**(3), 263.

35. Y.-H. Li, S. Wang, Z. Luan, J. Ding, C. Xu and D. Wu, *Carbon*, 2003, **41**(5), 1057.

36. G. P. Rao, C. Lu and F. Su, *Separation and purification technology*, 2007, **58**(1), 224.

37. L. Qi, Z. Xu, X. Jiang, C. Hu and X. Zou, *Carbohydrate Research*, 2004, **339**(16), 2693.

38. A. Panáček, L. Kvitek, R. Prucek, M. Kolar, R. Vecerova, N. Pizurova, V. K. Sharma, T. Nevečná and R. Zboril, *The Journal of Physical Chemistry B*, 2006, **110**(33), 16248.

39. G. Ren, D. Hu, E. W. C. Cheng, M. A. Vargas-Reus, P. Reip and R. P. Allaker, *International journal of antimicrobial agents*, 2009, **33**(6), 587.

40. S. Kang, M. Herzberg, D. F. Rodrigues and M. Elimelech, *Langmuir*, 2008, **24**(13), 6409.

41. F. J. Cerino-Córdova, A. M. García-León, E. Soto-Regalado, M. N. Sánchez-González, T. Lozano-Ramírez, B. C. García-Avalos and J. A. Loredo-Medrano, *J. Environ. Manage.*, 2012, **95 Suppl**, S77-82.

42. S.-F. Wang, L. Shen, W.-D. Zhang and Y.-J. Tong, *Biomacromolecules*, 2005, **6**(6), 3067.

43. K. Ogawa, S. Hirano, T. Miyanishi, T. Yui and T. Watanabe, *Macromolecules*, 1984, **17**(4), 973.

44. T. Theivasanthi and M. Alagar, *arXiv preprint arXiv:1003.6068*, 2010.

45. D. Tiwari, *Water Environment Research*, 2011, **83**(9), 874.

46. Cerino-Córdova, F de J, Am García-León, E. Soto-Regalado, M. N. Sánchez-González, T. Lozano-Ramírez, B. C. García-Avalos and J. A. Loredo-Medrano, *Journal of environmental management*, 2012, **95**, S77.

47. V. Vadivelan and K. V. Kumar, *Journal of Colloid and Interface Science*, 2005, **286**(1), 90.

48. K. C. Justi, V. T. Fávere, M. Laranjeira, A. Neves and R. A. Peralta, *Journal of Colloid and Interface Science*, 2005, **291**(2), 369.

49. H. L. Vasconcelos, T. P. Camargo, N. S. Gonçalves, A. Neves, M. Laranjeira and V. T. Fávere, *Reactive and Functional Polymers*, 2008, **68**(2), 572.

50. J. Febrianto, A. N. Kosasih, J. Sunarso, Y.-H. Ju, N. Indraswati and S. Ismadji, *Journal of Hazardous Materials*, 2009, **162**(2), 616.

51. W. S. Wan Ngah, A. Kamari and Y. J. Koay, *International Journal of Biological Macromolecules*, 2004, **34**(3), 155.

52. S. S. Tripathy and A. M. Raichur, *Journal of Hazardous Materials*, 2008, **153**(3), 1043.

53. A.-H. Chen, S.-C. Liu, C.-Y. Chen and C.-Y. Chen, *Journal of Hazardous Materials*, 2008, **154**(1), 184.

54. A. Özcan, A. S. Özcan, S. Tunali, T. Akar and I. Kiran, *Journal of Hazardous Materials*, 2005, **124**(1), 200.

55. N. Ünlü and M. Ersoz, *Journal of Hazardous Materials*, 2006, **136**(2), 272.

56. S.-J. Park and Y.-M. Kim, *Materials Science and Engineering: A*, 2005, **391**(1), 121.

57. H. J. Michael and I. S. Ayebaemi, *African Journal of Biotechnology*, 2005, **4**(2), 191.

58. C. Gabaldón, P. Marzal, J. Ferrer and A. Seco, *Water Research*, 1996, **30**(12), 3050.

59. A. Üçer, A. Uyanik and Ş. F. Aygün, *Separation and purification technology*, 2006, **47**(3), 113.

60. P. Trivedi, L. Axe and J. Dyer, *Colloids and Surfaces A: Physicochemical and Engineering Aspects*, 2001, **191**(1), 107.

61. F. Ruowen, Z. Hanmin and L. Yun, *Carbon*, 1993, **31**(7), 1089.

Metal	Material	Pseudo 1st order		1st order		Pseudo 2nd order			2nd order	
		R^2	K_{p1}	R^2	K_1	R^2	q_e	K_{p2}	R^2	K_2
Cu(II)	Chitosan	3.300e-3	3.454e-3	5.900e-3	-2.614	0.995	-0.042	7.820e-3	0.027	3.300e-3
	Multifunctional composite	0.109	0.010	0.193	-1.689	0.999	-0.029	1.100e-3	1.000e-3	0.109
Cd(II)	Chitosan	0.160	0.0152	0.080	-1.566	0.947	7.585e-3	2.000e-3	-1.200e-3	0.160
	Multifunctional composite	0.117	-0.059	0.552	-9.686	1.000	2.356	0.534	-2.082	0.117
Pb(II)	Chitosan	0.014	4.606e-3	3.600e-3	-2.178	0.927	-0.035	0.055	9.500e-3	0.0148
	Multifunctional composite	0.042	0.003	0.118	-1.126	0.982	35.71	0.006	0.091	0.007

Table 1: Kinetics parameters for Cu (II), Cd (II), Pb (II) ions adsorption.

Isotherm	Material	Chitosan	Multifunctional composite
Langmuir	$q_{max, cal}$	14.4	70.4
	K_L x 10^3	394	4.26
	R^2 (Linear form)	0.99	0.28
	R^2 (Non-linear form)	0.90	0.99
Freundlich	K_f	-0.07	0
	n	6.05	1.06
	R^2 (Linear form)	0.96	0.96
	R^2 (Non-linear form)	0.95	0.99
Temkin	K_T	28.3	7.38
	B_T	1.87	6.57
	R^2 (Linear form)	0.94	0.96
	R^2 (Non-linear form)	0.97	0.98
D-R model	k	1e-6	5e-5
	q_m	12.8	11.4
	E	100	714.85
	R^2 (Linear form)	0.74	0.86

Table 2: Isotherms parameters of Cu (II) adsorption on chitosan and the multifunctional composite.

Material	Ionic radius	Electronegativity	E^o	Ionization Energy	Polarizability	R$_H$
Chitosan	0.078	0.201	0.988	0.419	0.917	0.917
Multifunctional composite	0.891	0.841	3.09e-3	0.528	0.056	0.056

Table 3: R^2 values of the relation between the maximum uptake capacity and the electrochemical parameters of the used metal ions.
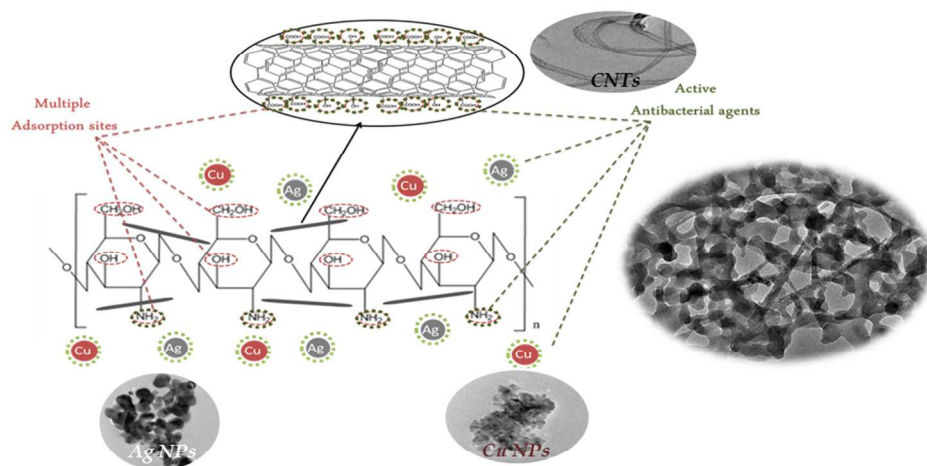
Chitosan/Ag NPs/Cu NPs/CNTs multifunctional composite has a superior water treatment efficiency than the bare chitosan and the bi-composites systems

Graphical abstract
275x190mm (96 x 96 DPI)
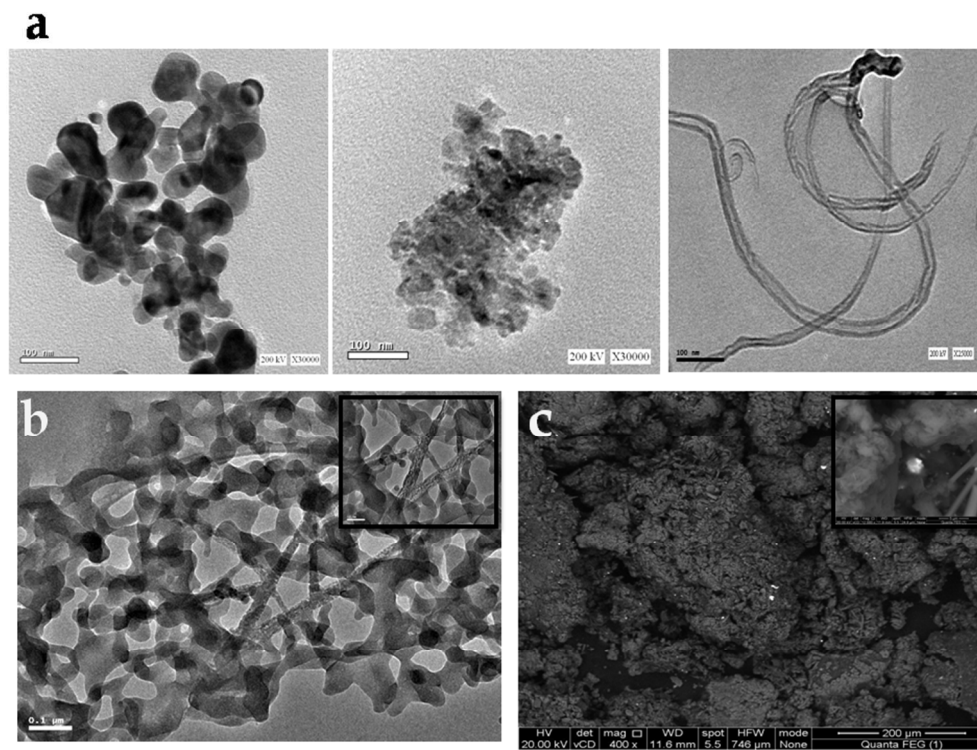
Figure 1a) TEM images of Ag NPs (right) Cu NPs (middle) and MWCNTs (left), b) TEM image of the multifunctional composite; the insertion is for higher magnification image and c) SEM image of the multifunctional composite; the insertion is for higher magnification image.
254x190mm (96 x 96 DPI)
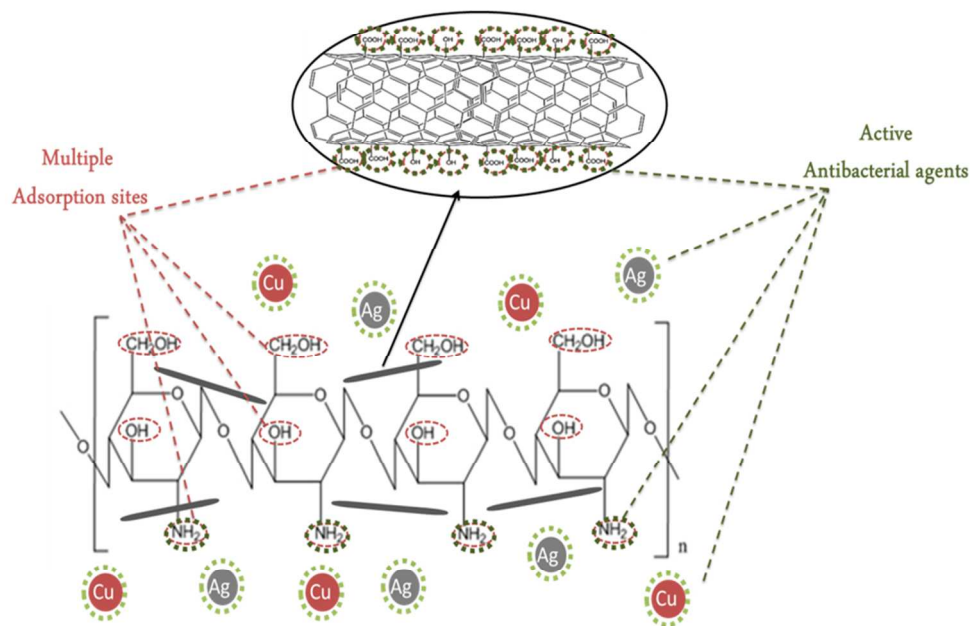
Scheme 1: Schematic representation of the different active sites of the prepared multifunctional composite.
254x190mm (96 x 96 DPI)
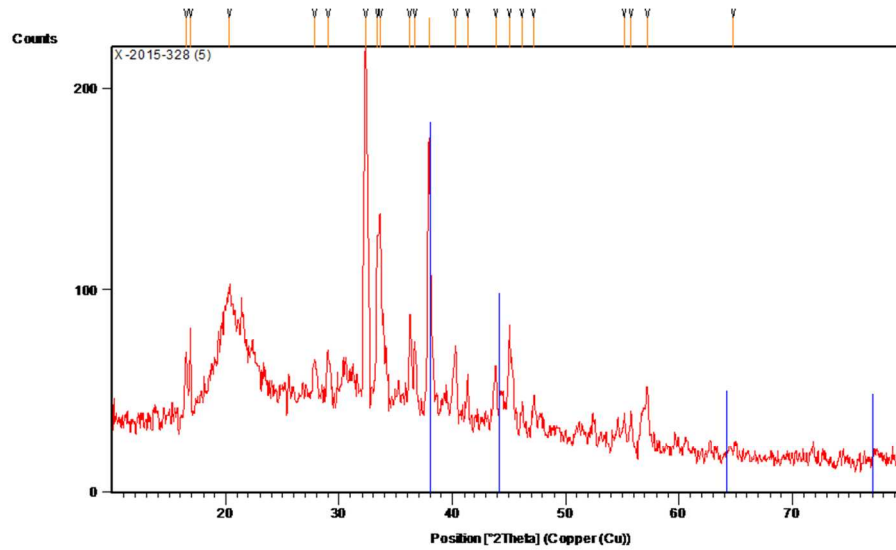
Figure 2: XRD of the prepared multifunctional composite.
254x190mm (96 x 96 DPI)
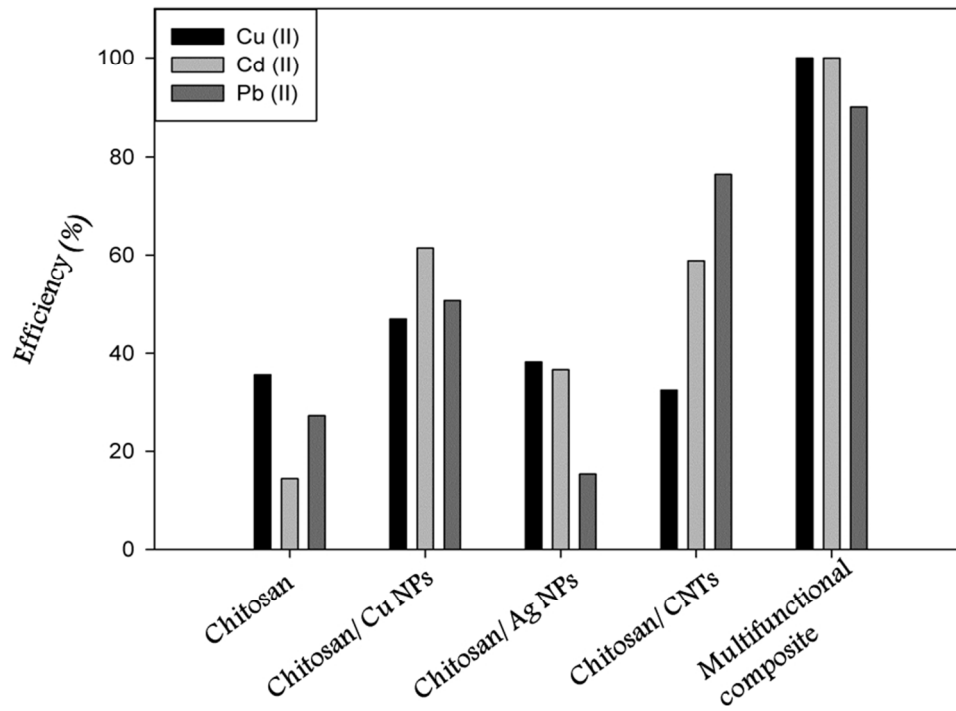
Figure 3: comparison study of the uptake capacity of chitosan, chitosan/Cu NPs nanocomposite, chitosan/Ag NPs nanocomposite, chitosan/CNTs nanocomposite and chitosan/ Ag NPs/ Cu NPs/CNTs multifunctional composite regarding Cu(II), Cd(II) and Pb(II)metal ions (100 ppm, 1h, 3 g/L).
254x190mm (96 x 96 DPI)
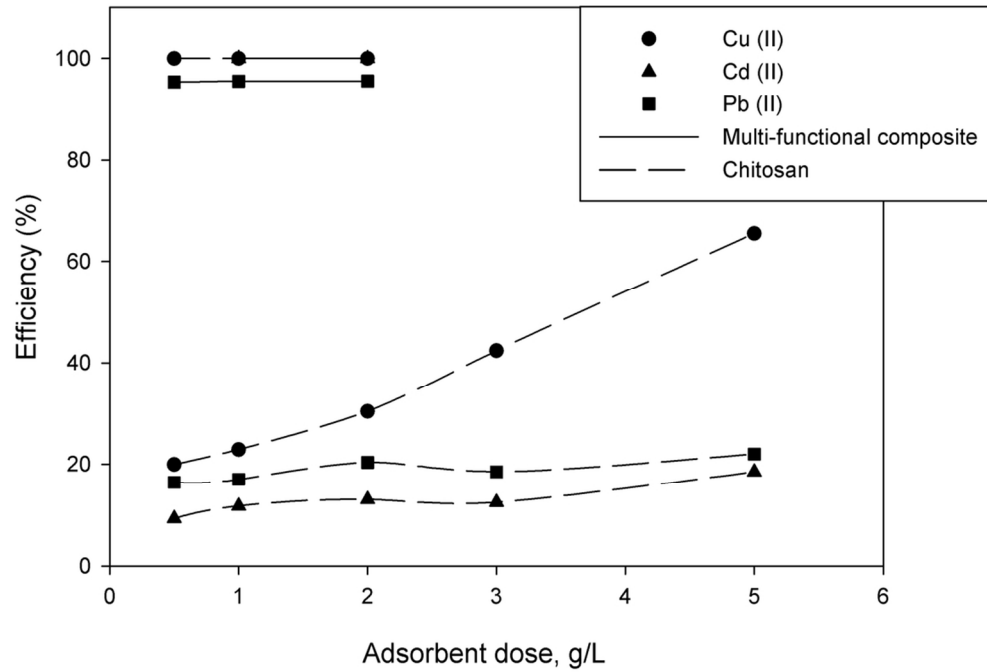
Figure 4: Effect of adsorbent dose of chitosan and the multifunctional composite keeping the concentration at 100ppm for 60min.
99x77mm (300 x 300 DPI)
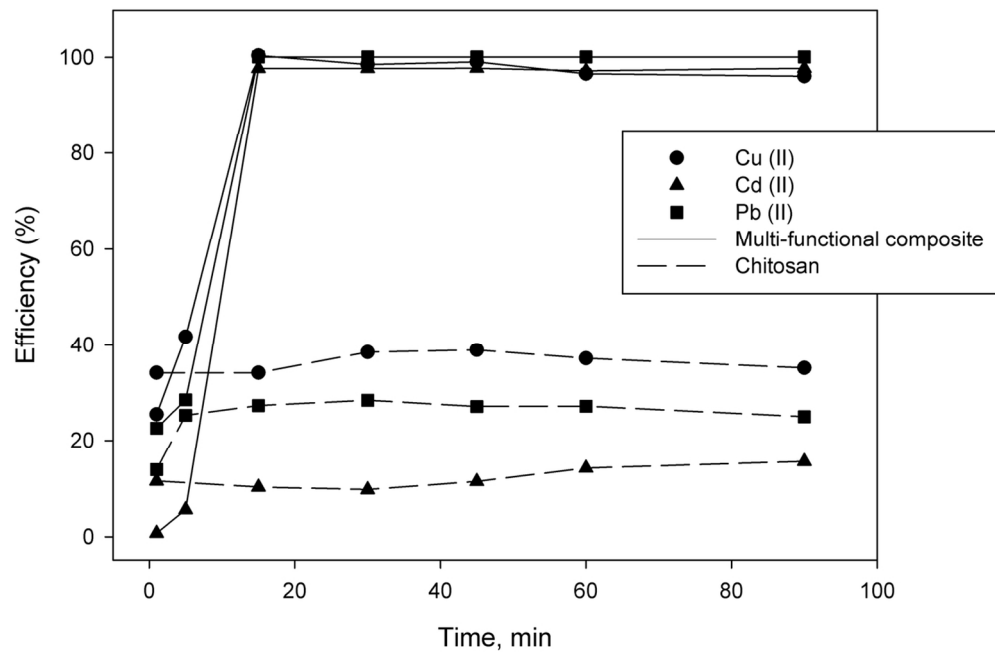
Figure 5: Uptake capacity of the multifunctional composite over time (3g/L, 100ppm).
119x87mm (300 x 300 DPI)
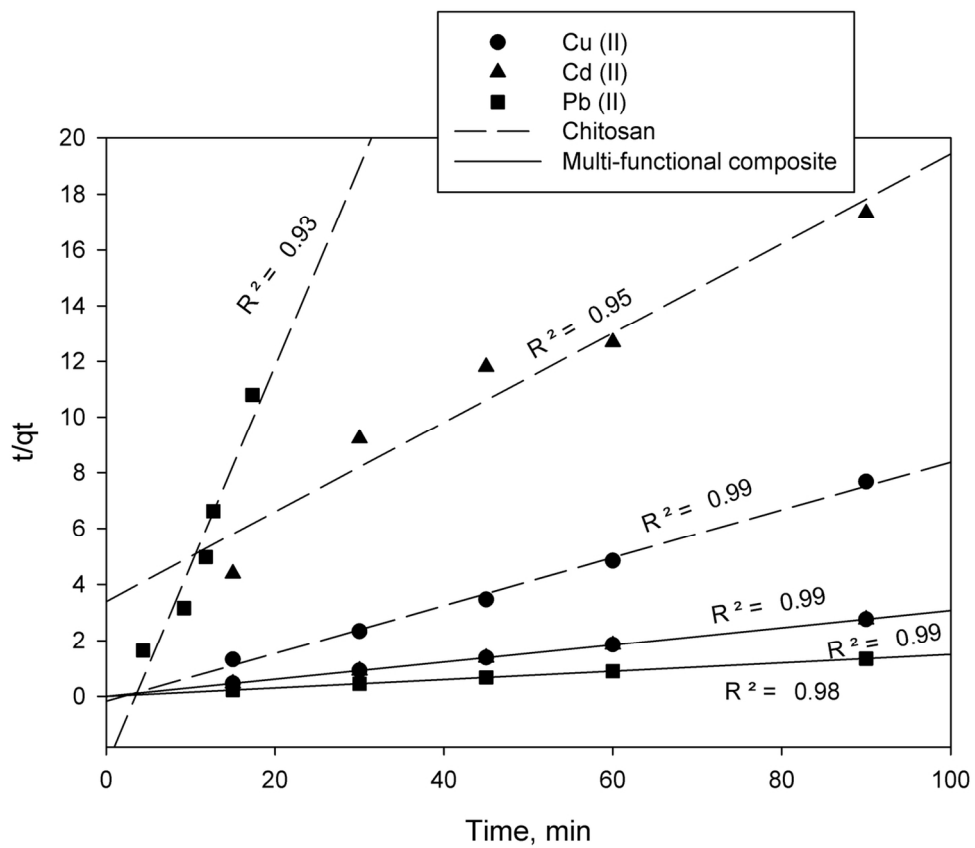
Figure 6: Adsorption kinetics pseudo-second order model of Cu(II), Cd(II) and Pb(II) ions on chitosan and the multifunctional composite.
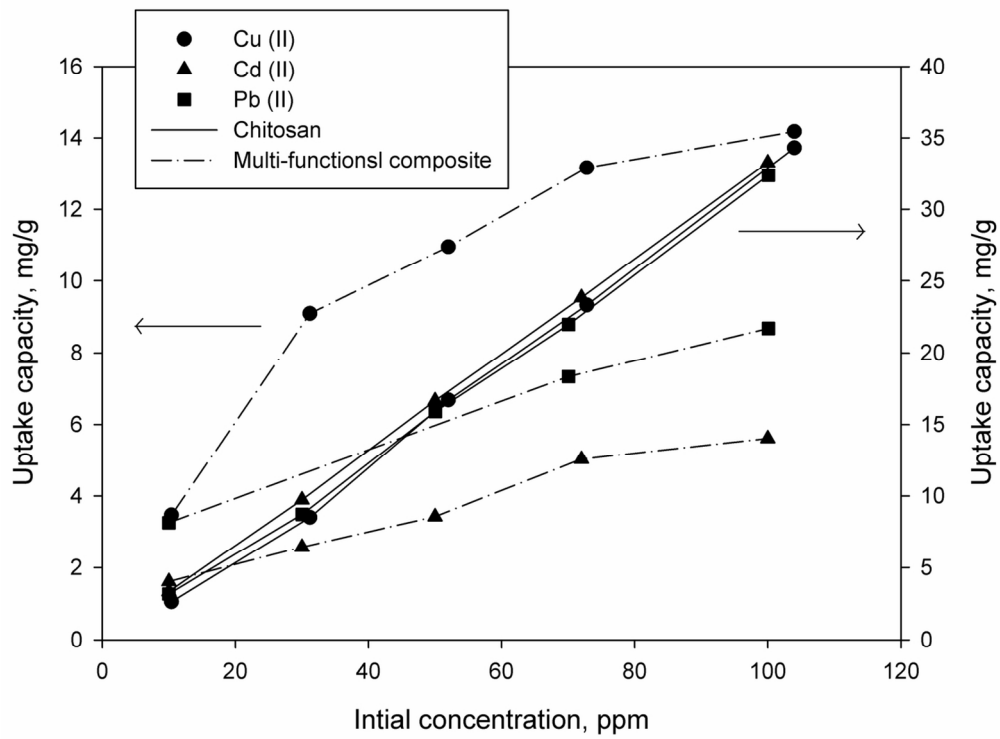125x106mm (300 x 300 DPI)

Figure 7: Effect of initial concentration of Cu(II), Cd(II) and Pb(II) ions on chitosan and multifunctional composite uptake capacity(3g/L, 60min).
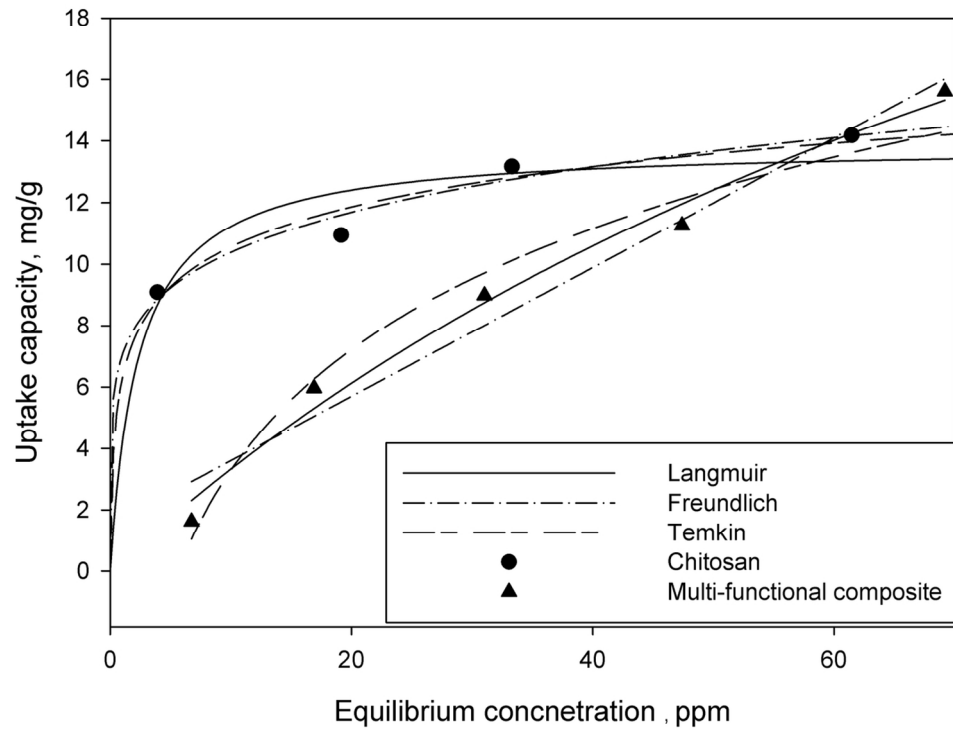119x91mm (300 x 300 DPI)

Figure 8: Cu(II) adsorption isotherms fitting of chitosan and multifunctional composite (3g/L, 60min).
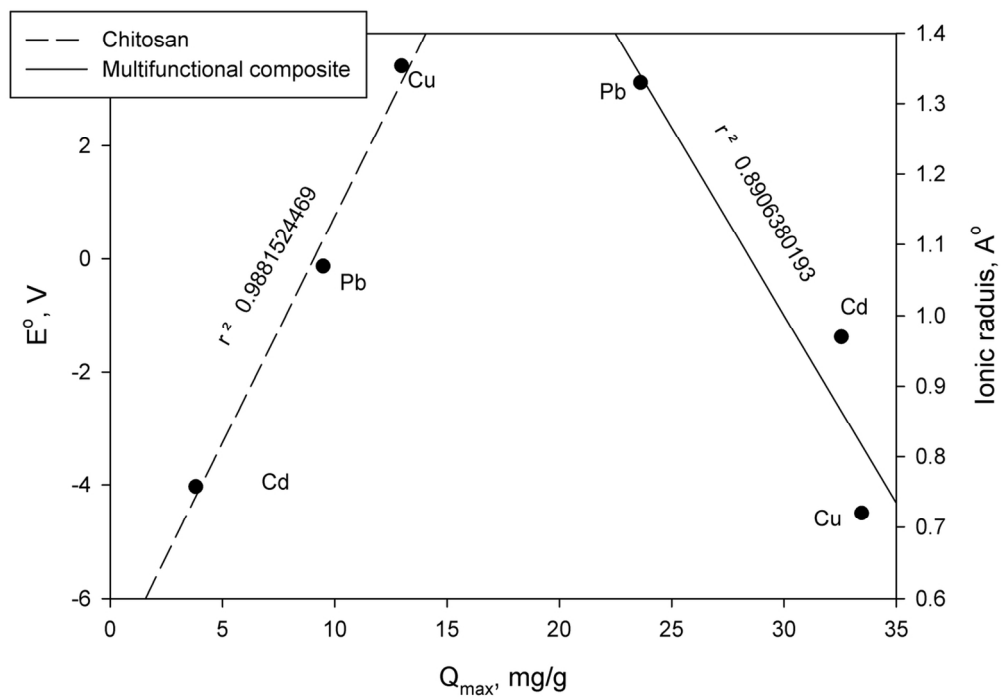119x96mm (300 x 300 DPI)

Figure 9: The most fitted electrochemical parameters of Cu(II), Cd(II) and Pb(II) in relation to maximum uptake capacity of chitosan and the multifunctional composite.
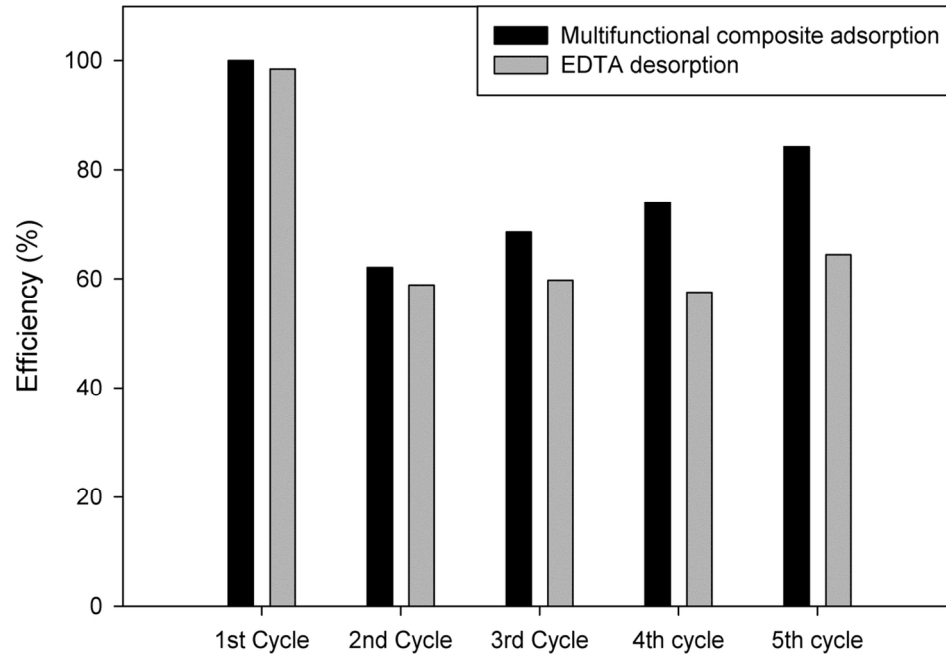120x92mm (300 x 300 DPI)

Figure 10: Adsorption / desorption cycles of the multifunctional composite using Cu (II) as adsorbate and EDTA as eluting agent.
114x88mm (300 x 300 DPI)